Aalto University

Aaltodoc

OPEN ACCESS

Author(s): Karvonen, Lasse & Alasaarela, Tapani & Jussila, Henri & Mehravar, Soroush & Chen, Ya & Säynätjoki, Antti & Norwood, Robert A. & Peyghambarian, Nasser & Kieu, Khanh & Honkanen, Seppo & Lipsanen, Harri

Title: Nanolaminate structures fabricated by ALD for reducing propagation losses and enhancing the third-order optical nonlinearities

Year: 2014

Version: Final published version

Please cite the original version:

Nanolaminate structures fabricated by ALD for reducing propagation losses and enhancing the third-order optical nonlinearities

Lasse Karvonen[a,*], Tapani Alasaarela[a], Henri Jussila[a], Soroush Mehravar[b], Ya Chen[a], Antti Säynätjoki[a], Robert A. Norwood[b], Nasser Peyghambarian[b], Khanh Kieu[b], Seppo Honkanen[c], and Harri Lipsanen[a]

[a]Aalto University, School of Electrical Engineering, Department of Micro and Nanosciences, P.O. Box 13500, FI-00076 Aalto, Finland
[b]University of Arizona, College of Optical Sciences, 1630 E University Blvd., Tucson, AZ 85721, USA
[c]University of Eastern Finland, Department of Physics and Mathematics, P.O. Box 111, FI-80101 Joensuu, Finland
[*]lasse.karvonen@aalto.fi

ABSTRACT

We demonstrate a novel atomic layer deposition (ALD) process to make high quality nanocrystalline titanium dioxide (TiO_2) and zinc oxide (ZnO) with intermediate Al_2O_3 layers to limit the crystal size. The waveguide losses of TiO_2/Al_2O_3 nanolaminates measured using the prism coupling method for both 633 nm and 1551 nm wavelengths are as low as 0.2 ± 0.1 dB/mm with the smallest crystal size. We also show that the third-order optical nonlinearity in ZnO/Al_2O_3 nanolaminates can be enhanced by nanoscale engineering of the thin film structure.

Keywords: atomic layer deposition, loss, third-order optical nonlinearity

1. INTRODUCTION

Nanoscale materials often exhibit remarkable differences in mechanical, optical and electrical properties compared to their bulk form[1,2]. Fabrication of these structures in a controlled fashion can be challenging. Therefore, a simple method to controllably fabricate these nanoscale structures is important. Atomic layer deposition (ALD) has been used to fabricate nanolaminate structures, for instance from aluminum and zinc oxide (Al_2O_3 and ZnO) layers[3,4].

Aluminum doped zinc oxide (AZO) is a material that has been intensively studied mainly because of its application as a transparent conducting electrode[5-7]. Furthermore, zinc oxide is also an interesting material because of its outstanding nonlinear optical properties[8-13]. The third-order optical nonlinearity, $\chi^{(3)}$, is important for many applications in optical signal processing and telecommunications. For example, the large $\chi^{(3)}$ in silicon has already enabled impressive device demonstrations, e.g., wavelength conversion, all-optical switching and optical signal processing at low optical power levels[14-16]. Silicon has a high $\chi^{(3)}$, but two-photon absorption related to the imaginary part of $\chi^{(3)}$ limits its usefulness. We have earlier shown that ALD grown Al_2O_3 and titanium dioxide TiO_2 work well with silicon slot and strip waveguides[17-20]. TiO_2 is a promising material for linear and nonlinear microphotonic devices at both visible and infrared wavelengths. Previously, atomic layer deposition (ALD), reactive radio frequency magnetron sputtering, sol-gel and ion implantation methods have been studied as potential methods to make low loss TiO_2 waveguides[21-26].

Titanium dioxide thin films can appear in many different crystalline phases and the phase is mainly dependent on the growth temperature and/or annealing temperature, but also on the surface on which it grows[27]. The lowest losses are measured for amorphous TiO_2 waveguides, but they are thermally unstable as the films crystallize when heated to > 200°C[28]. This can limit their applicability in applications requiring higher temperature steps during the fabrication process. Furthermore, amorphous TiO_2 is less nonlinear than its crystalline anatase or rutile counterparts. Thus, TiO_2 films deposited at higher temperature but still having low losses would be highly desirable in various optical

applications. ALD provides a straightforward way to fabricate nanolaminates while controlling the crystal size at the nanometer scale. Crystal size control has been used previously to improve the optical properties and uniformity when TiO_2 is deposited at higher temperature[29,30].

The diethyl zinc (DEZn) + water process for ZnO, the titanium chloride ($TiCl_4$) + water process for TiO_2 and the trimethylaluminum (TMA) + water process for Al_2O_3 are very widely used ALD processes as the precursors are liquid and have suitable vapor pressures for evaporation at ambient temperature. In addition the processes have large ALD temperature windows in which they can be utilized. However, when the $TiCl_4$ + water and TMA + water processes are combined the layer interfaces tend to have high optical absorption[21], an effect which has been utilized to create absorbing decorative coatings using the H_2O + $TiCl_4$ + TMA –process[31]. TiO_2 crystal growth termination via Al_2O_3 has been done using different chemistries, e.g. the $AlCl_3$ + H_2O process, but these precursors are not as ideal ALD precursors as TMA[30]. Therefore, we used the TMA + ozone process and observed that it is working well with the $TiCl_4$ + water process[32].

2. NANOLAMINATE STRUCTURES
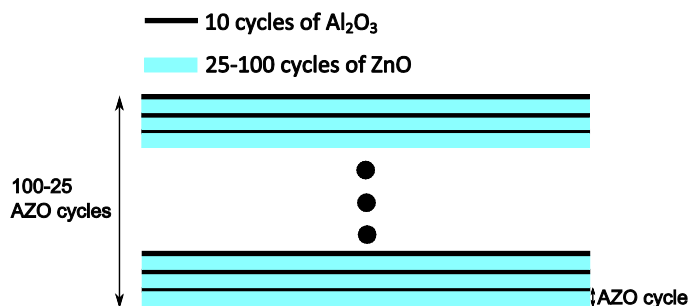
ZnO/Al$_2$O$_3$ nanolaminates

Fig. 1. Schematic diagram of the ZnO/Al$_2$O$_3$ nanolaminate structure.

Four ZnO/Al_2O_3 nanolaminate samples and one plain ZnO film were prepared by a Beneq TFS 500 ALD system on Corning 0211 glass substrates. The schematic diagram of the nanolaminate structure is shown in Fig. 1. The ZnO/Al_2O_3 nanolaminates consist of alternating layers of ZnO and Al_2O_3. The thickness of each layer is defined by the number of ALD cycles. We kept the total number of ZnO growth cycles constant in all samples to ensure equal amounts of ZnO. Since the number of Al_2O_3 and ZnO layers varies, the number of cycles in each ZnO layer was changed from 25 to 100 depending on the sample (see table 1.). All Al_2O_3 layers in the nanolaminates were formed with 10 ALD cycles (thickness of about 1.1 nm). Diethyl zinc (DEZn) and H_2O acted as precursors for ZnO and trimethyl aluminum (TMA) and H_2O for Al_2O_3[33], and the growth temperature was 200 °C. Sample labeling is presented in Table 1.

Table 1. Labeling of the ZnO/Al$_2$O$_3$ nanolaminate samples

Sample name	Number of AZO cycles	An AZO cycle consists of	
		Number of Al$_2$O$_3$ cycles	Number of ZnO cycles
AZO1	100	10	25
AZO2	50	10	50
AZO3	33	10	75
AZO4	25	10	100
ZNO	1	0	2500

TiO$_2$/Al$_2$O$_3$ nanolaminates

TiO$_2$/Al$_2$O$_3$ nanolaminates (samples S0-S4) were fabricated using $TiCl_4$ + H_2O and TMA + O_3 ALD processes at a growth temperature of 250 °C. The growth rate of the TMA + O_3 process is reported to be between 0.09 to 0.11 nm/cycle[34,35]. Therefore, the Al_2O_3 layer thickness is estimated to be about 1 nm. Fabricated samples are presented in

Table 2. The structure of these samples is very similar to that of the ZnO/Al$_2$O$_3$ nanolaminates. Sample S5 is fabricated using the TiCl$_4$ + H$_2$O process at 120 °C and sample S6 is sample S5 annealed at 400 °C for crystallizing the film.

Table 2. Naming of the TiO$_2$/Al$_2$O$_3$ nanolaminate samples.

Sample name	Number of TiO$_2$+Al$_2$O$_3$ cycles	An TiO$_2$+Al$_2$O$_3$ cycle consists of	
		Number of TiO$_2$ cycles	Number of Al$_2$O$_3$ cycles
S0	1	4000	0
S1	40	100	11
S2	20	200	11
S3	15	267	11
S4	10	400	11
S5	1	~3300	0
S6 (annealed S5 at 400 °C)	1	~3300	0

3. RESULTS AND DISCUSSION

3.1. Optical properties

ZnO/Al$_2$O$_3$ nanolaminates

The effective refractive index and the total thickness of each sample were measured using a prism coupler at the wavelengths of 532 nm, 633 nm and 1551 nm. The measured effective refractive indices are shown in Fig. 2.
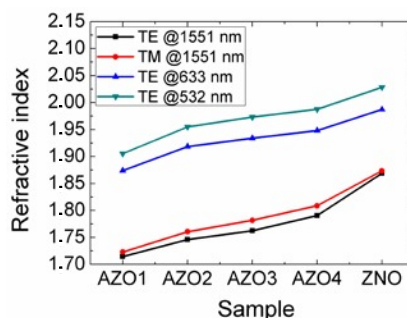

Fig. 2. Measured refractive indices of the ZnO/Al$_2$O$_3$ nanolaminate and ZnO samples.

Table 3. Properties of the ZnO/Al$_2$O$_3$ nanolaminate samples.

Sample	Effective refractive index N	Total thickness t_{tot} (nm)	Estimated total ZnO thickness in nanolaminate (nm)	Estimated total Al$_2$O$_3$ thickness in nanolaminate (nm)
AZO1	1.87	516.7	339.9	176.8
AZO2	1.92	494.9	388.6	106.2
AZO3	1.93	478.9	398.0	80.9
AZO4	1.95	486.1	424.0	62.1
ZNO	1.99	501.4	501.4	0

The results of the measurement at 633 nm are shown in Table 3. The estimated total and layer thicknesses of ZnO and Al$_2$O$_3$ in nanolaminates are also shown in Table 3. They are calculated from the measured effective refractive indices using the equation $t_h = \frac{(N^2 - n_l^2)}{(n_h^2 - n_l^2)} t_{tot}$, where t_h, t_l, n_h and n$_l$ are the high-index (ZnO, n_h = 1.99) and low-index (Al$_2$O$_3$, n_l = 1.63) materials' thicknesses and refractive indices, and t_{tot} and N are the nanolaminate thickness and effective refractive index, respectively[36]. Here we assume that the refractive index of ZnO is constant regardless of the layer thickness. We

measured the linear absorbance of our samples using an untreated Corning 0211 glass plate as a reference. The obtained spectra are presented in Fig. 3a. For the ZnO sample, a sharp absorption edge is observed at the wavelength 375 nm, corresponding to the bandgap of ZnO. For the nanolaminate samples, the absorbance below the absorption edge decreases with decreasing amount of ZnO. The absorbance data at 350 nm (shown in Fig. 3b) agrees well with our estimations (Table 3) of the total amount of ZnO in the samples.
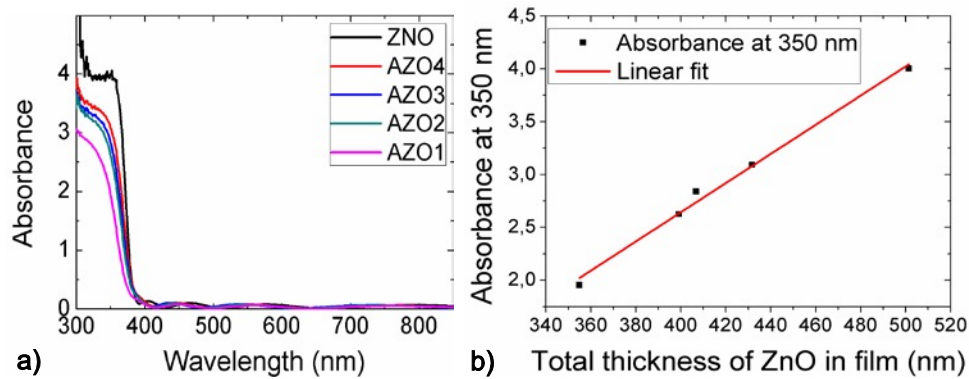

Fig. 3. a) Measured absorption spectra of the samples, and b) absorption at 350 nm as a function of the estimated amount of ZnO.

TiO$_2$/Al$_2$O$_3$ nanolaminates

Table 4. Estimated loss values of TiO$_2$/Al$_2$O$_3$ nanolaminates and TiO$_2$ films.

Sample	Loss at 633 nm [dB/mm]	Loss at 1551 nm [dB/mm]
S0	very high	very high
S1	0.2 ± 0.1	0.2 ± 0.1
S2	0.6 ± 0.1	0.2 ± 0.1
S3	very high	0.8 ± 0.1
S4	very high	1.0 ± 0.1
Amorphous TiO$_2$ (similar as S5)	0.2-0.35[21]	0.08-0.09[21]

Propagation losses of the TiO$_2$/Al$_2$O$_3$ nanolaminates and the TiO$_2$ reference sample were estimated using the loss measurement feature of the prism coupler at the wavelengths of 633 and 1551 nm. The measured losses are presented in Table 4. The loss values are decreasing when the TiO$_2$ sublayer thickness decreases. The lowest value, 0.2 dB/mm at both wavelengths, was measured from the sample S1. Higher loss values at the wavelength of 633 nm can be explained by higher scattering from the small crystals. In Rayleigh scattering, the scattering intensity is inversely proportional to the fourth power of the wavelength. Therefore, the scattering from the small particles (crystals in this case) is increasing when the wavelength is decreasing; deviation from the Rayleigh law can be due to the presence of larger particles that would exhibit Mie scattering. The loss value of 2 dB/cm is very promising for waveguiding applications. The loss of amorphous ALD TiO$_2$ grown at 120 °C has been reported to be less than 1 dB/cm[21]. However, the nanolaminate structure is much more stable thermally than low temperature TiO$_2$.

3.2. Crystal structure

ZnO/Al2O3 nanolaminates

In order to characterize the crystal structure and the size of the crystallites in the ZnO layers, powder X-ray diffraction (XRD) experiments using Cu K-α radiation were carried out. The measured XRD curves are shown in Fig. 4a. Diffraction peaks are located at positions 31.8°, 34.4°, 56.6° and 66.4° corresponding to (100), (002), (110) and (200) crystal planes of hexagonal wurtzite ZnO. The peak at 31.8° comes from *a*-direction oriented crystals and the peak at 34.4° from *c*-direction oriented crystals[37,38]. These results indicate *c*-direction oriented ZnO crystals in the beginning of the growth, but for the thicker films *a*-direction oriented growth begins to dominate. ZnO, grown using ALD at 200 °C

with the same precursors, has been earlier reported to be *a*-direction oriented[37]. Crystallite sizes estimated using Scherrer's formula are presented in Fig. 4b. These results show that an approximately 2 nm thick amorphous Al_2O_3 layer between ZnO layers terminates the ZnO crystal growth and affects the size of the crystallites in the nanolaminates.
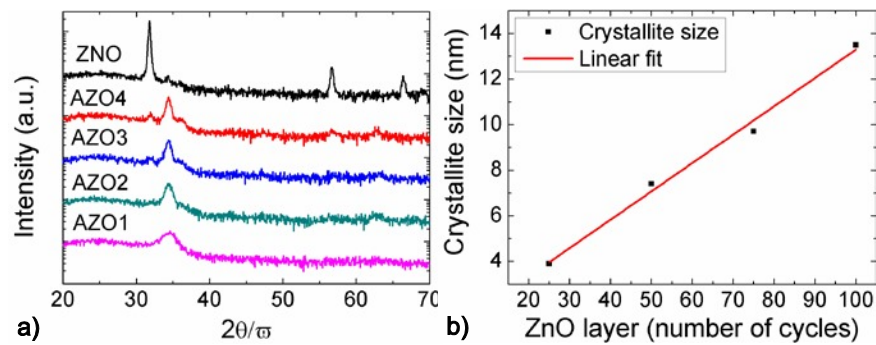

Fig. 4. a) Measured powder XRD curves and b) calculated crystallite sizes of the samples.

Top view scanning electron micrographs are presented in Fig. 5. In the ZNO sample, the crystals are very large compared to the AZO samples and their shape is more like elongated than spherical as is the case with the AZO films. The crystal size clearly increases from AZO1 to AZO4 as the XRD results suggest. However, the smallest crystals seem larger than the lower bound estimated from the XRD peak width.
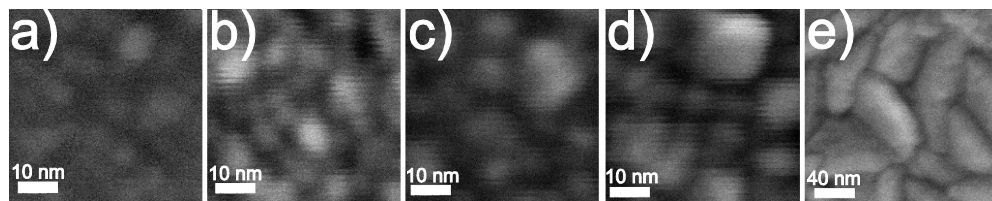

Fig. 5. Top view SEM images of the samples: a) AZO1, b) AZO2, c) AZO3, d) AZO4, and e) ZNO.

TiO₂/Al₂O₃ nanolaminates

In order to characterize the crystal structure and the size of the crystallites in the TiO_2/Al_2O_3 nanolaminates, similar powder XRD experiments were carried out. Measured XRD curves of the TiO_2/Al_2O_3 nanolaminates are shown Fig. 6a. Diffraction peaks are located at the positions 25.3°, 48.0°, and 55.1°, which correspond to (101), (200), and (211) planes of anatase TiO_2, respectively. These results indicate that the grown TiO_2 is in the anatase phase in samples S0, S3, and S4. The samples S1, and S2 do not show visible peaks in the XRD suggesting the amorphous phase. Fig. 6b shows the top view SEM images of the samples SO-S4. S1 and S2 look like amorphous film without any clear crystals. Large crystals are seen in the samples S0 and S4. Smaller crystals can be found from S3.
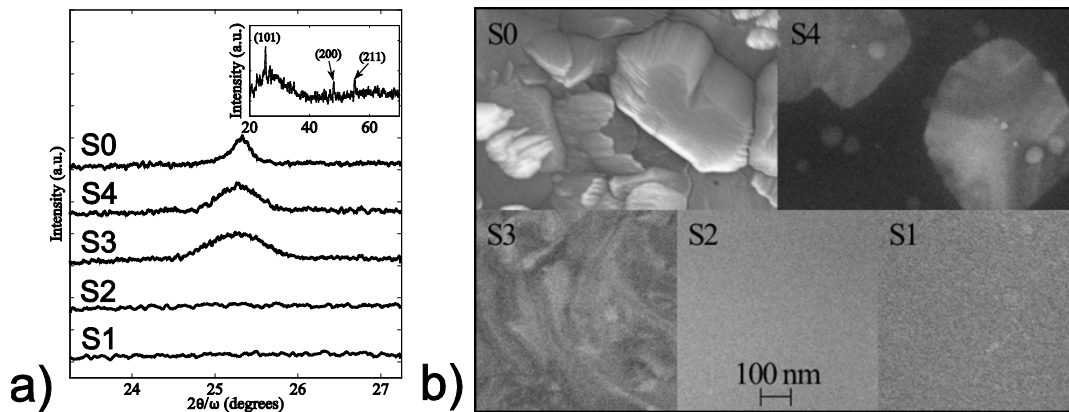
Fig. 6. a) Measured XRD curves and b) top view SEM images of the TiO_2/Al_2O_3 samples.

3.3. Third-order optical nonlinearity

ZnO/Al₂O₃ nanolaminates

The third-order optical nonlinearity of the nanolaminates was characterized using a multiphoton microscope. The third harmonic generation (THG) signal as a function of crystallite size is plotted in Fig. 7a. The figure shows that the THG signal increases almost linearly as the crystallite size decreases. We assume that the THG is mainly from ZnO because the third-order optical nonlinearity coefficient $\chi^{(3)}$ of Al_2O_3 has been reported to be about 20 times less than in ZnO[9]. AZO1 sample generates 13 times higher THG signal than a homogeneous ZnO sample. THG is proportional to $(V \cdot \chi^{(3)})^2$ where $\chi^{(3)}$ is the third-order optical nonlinearity coefficient and V is the material volume. The estimated $\chi^{(3)}$ of the nanolaminate samples normalized to ZnO film are presented in Fig. 7b. We also measured the THG signal from Corning 0211 glass as a reference and the value was 2.26. Therefore, the THG signal from the nanolaminate with the smallest crystals is about 200 times stronger than from glass. Aluminum doped zinc oxide is a well-known transparent conducting oxide. We also observed that zinc oxide was doped by aluminum in our nanolaminates even though our Al_2O_3 sublayers are relatively thick. Therefore, one explanation for the higher third-order nonlinearities from AZO1 and AZO2 samples could be that they contain more free electrons than ZNO, AZO4 and AZO3.
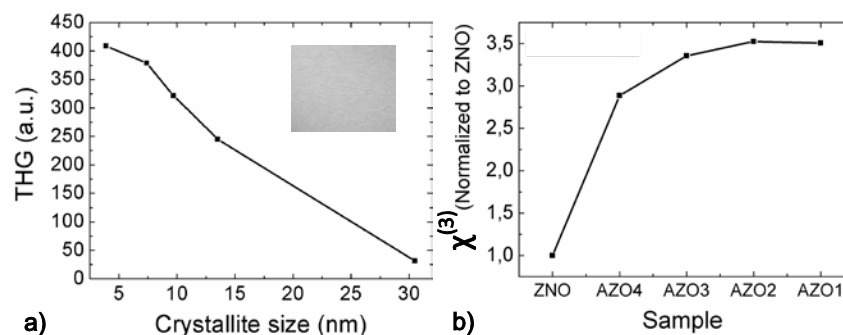

Fig. 7. a) THG signal as a function of crystallite size and b) $\chi^{(3)}$ of the samples normalized to ZNO sample. Inset in a) shows the 50x50 μm^2 THG signal image from the sample AZO1.

TiO₂/Al₂O₃ nanolaminates

Thicknesses of the samples and the measured THG signals are presented in Table 5. Thicknesses are estimated using a spectral transmission measurement. The highest THG signal was observed from the crystalline TiO_2 reference sample. The highest THG signal measured from the TiO_2/Al_2O_3 nanolaminates was from the sample S4 which has the largest crystals and the smallest number of interfaces. We believe that this is due to the larger amount of anatase TiO_2. The

sample S2 seems to be the best trade-off having almost two thirds of the THG signal compared to S0, but still having low losses at the wavelength of 1551 nm (2 dB/cm). If we take thickness into account then it looks like that the sample S4 has the highest $\chi^{(3)}$. Also the sample S1 has still relatively high $\chi^{(3)}$ compared to the amorphous TiO$_2$ (sample S5).

Table 5. Thicknesses and THG signals of S0-S6 samples.

Sample	Thickness (nm)	THG signal (normalized to S0)	$\chi^{(3)}$ (normalized to S0)
S0	203 ± 10	1 ± 0.08	1
S1	195 ± 2	0.46 ± 0.08	0.70
S2	183 ± 2	0.66 ± 0.08	0.90
S3	173 ± 2	0.76 ± 0.08	1.02
S4	168 ± 2	0.80 ± 0.08	1.08
S5	200 ± 2	0.57 ± 0.08	0.44
S6	200 ± 2	0.72 ± 0.08	0.76

4. CONCLUSIONS

We demonstrated the novel atomic layer deposition (ALD) process to control the crystallinity of titanium dioxide (TiO$_2$) and zinc oxide (ZnO) using amorphous intermediate Al$_2$O$_3$ layers[4,32]. The waveguide losses of TiO$_2$/Al$_2$O$_3$ nanolaminates measured using prism coupling method for both 633 nm and 1551 nm wavelengths were as low as 0.2 ± 0.1 dB/mm with the thinnest TiO$_2$ layer. In comparison, plain TiO$_2$ deposited at 250°C without the intermediate Al$_2$O$_3$ layers shows high scattering losses and is not viable as a waveguide material. The third-order optical nonlinearity in TiO$_2$/Al$_2$O$_3$ nanolaminate was also studied, and it was shown that the crystallinity controlled ALD-TiO$_2$ is an excellent candidate for various optical applications, where good thermal stability and high third-order optical nonlinearity are needed. We also investigated the third-order optical nonlinearity in ZnO/Al$_2$O$_3$ nanolaminates fabricated by atomic layer deposition and showed that the third-order optical nonlinearity can be enhanced by nanoscale engineering of the thin film structure. The grain size of the polycrystalline ZnO film is controlled by varying the thickness of the ZnO layers in the nanolaminate. Nanoscale engineering enables us to achieve a third harmonic generated signal enhancement of ~13 times from the optimized nanolaminate structure compared to a ZnO reference film of comparable thickness.

5. ACKNOWLEDGEMENTS

6. REFERENCES

[1] Chang, Q., Ye, H. and Song, Y., "Effects of host and particle shape on the optical nonlinearities of nanocomposites," Colloids Surf. A, 298(1-2), 58-62 (2007).

[2] Zou, B. S., Volkov, V. V. and Wang, Z. L. "Optical properties of amorphous ZnO, CdO, and PbO nanoclusters in solution," Chem. Mater. 11(11), 3037-3043 (1999).

[3] Raghavan, R., Bechelany, M., Parlinska, M., Frey, D., Mook, W. M., Beyer, A., Michler, J. and Utke, I., "Nanocrystalline-to-amorphous transition in nanolaminates grown by low temperature atomic layer deposition and related mechanical properties" Appl. Phys. Lett. 100(19), 191912 (2012).

[4] Karvonen, L., Säynätjoki, A., Chen, Y., Jussila, H., Rönn, J., Ruoho, M., Alasaarela, T., Kujala, S., Norwood, R.A., Peyghambarian, N., Kieu, K., and Honkanen, S. "Enhancement of the third-order optical nonlinearity in ZnO/Al_2O_3 nanolaminates fabricated by atomic layer deposition," Appl. Phys. Lett., 103(3), 031903 (2013).

[5] Agura, H., Suzuki, A., Matsushita, T., Aoki, T. and Okuda, M., "Low resistivity transparent conducting Al-doped ZnO films prepared by pulsed laser deposition," Thin Solid Films 445(2), 263-267 (2003).

[6] Minami, T., "Transparent conducting oxide semiconductors for transparent electrodes," Semicond. Sci. Technol. 20(4), S35-S44 (2005).

[7] Dasgupta, N. D., Neubert, S., Lee, W., Trejo, O., Lee, J.-R., and Prinz, F. B., "Atomic layer deposition of Al-doped ZnO films: Effect of grain orientation on conductivity," Chem. Mater. 22(16), 4769-4775 (2010).

[8] Lin, J. H., Chen, Y. J., Lin, H. Y. and Hsieh, W. F., "Two-photon resonance assisted huge nonlinear refraction and absorption in ZnO thin films," J. Appl. Phys. 97(3), 033526 (2005).

[9] Adair, R., Chase, L. and Payne, S., "Nonlinear refractive index of optical crystals.," Physical review. B, Condensed matter 39(5), 3337–3350 (1989).

[10] Zhang, X. J., Ji, W. and Tang, S. H., "Determination of optical nonlinearities and carrier lifetime in ZnO," J. Opt. Soc. Am. B 14(8), 1951-1955 (1997).

[11] Johnson , J. C., Knutsen, K. P., Yan, H. Q., Law, M., Zhang, Y. F., Yang, P. D. and Saykally, R. J., "Ultrafast carrier dynamics in single ZnO nanowire and nanoribbon lasers," Nano Lett. 4(2), 197-204 (2004).

[12] Sun, C. K., Sun, S. Z., Lin, K. H., Zhang, K. Y. J., Liu, H. L., Liu, S. C. and Wu, J. J., "Ultrafast carrier dynamics in ZnO nanorods," Appl. Phys. Lett. 87(2), 023106 (2005).

[13] He, J., Qu, Y., Li, H., Mi, J., and Ji, W., "Three-photon absorption in ZnO and ZnS crystals," Opt. Express 13(23), 9235-9247 (2005).

[14] Kuo, Y.-H., Rong, H., Sih, V., Xu, S., Paniccia, M. and Cohen, O., "Demonstration of wavelength conversion at 40 Gb/s data rate in silicon waveguides," Opt. Express, 14(24), 11721-11726 (2006).

[15] Almeida, V. R., Barrios, C. A., Panepucci, R. R., Lipson, M., Foster, M. A., Ouzounov, D. G. and Gaeta, A. L., "All-optical switching on a silicon chip," Opt. Lett. 29(24), 2867-2869 (2004).

[16] Salem, R., Foster, M. A., Turner, A. C., Geraghty, D. F., Lipson, M. and Gaeta, A. L., "All-optical regeneration on a silicon chip," Opt. Express 15(12), 7802-7809 (2007).

[17] Alasaarela, T., Korn, D., Alloatti, L, Säynätjoki, A., Tervonen, A., Palmer, R., Leuthold, J., Freude, W., and Honkanen, S., "Reduced propagation loss in silicon strip and slot waveguides coated by atomic layer deposition," Opt. Express 19(12), 11529-11538 (2011).

[18] Säynätjoki, A., Karvonen, L., Hiltunen, M., Tu, X., Liow, T. Y., Tervonen, A., Lo, G. Q. and Honkanen, S., "Low-loss silicon slot waveguides and couplers fabricated with optical lithography and atomic layer deposition," Opt. Express 19(27), 26275-26282 (2011).

[19] Karvonen, L., Säynätjoki, A., Chen, Y., Tu, X., Liow, T. Y., Hiltunen, J., Hiltunen, M., Lo, G. Q., and Honkanen, S., "Low-loss multiple-slot waveguides fabricated by optical lithography and atomic layer deposition," IEEE Phot. Tech. Lett. 24(22), 2074-2076 (2012).

[20] Erdmanis, M., Karvonen, L., Säynätjoki, A., Tu, X., Liow, T. Y., Lo, G. Q., Vänskä, O., Honkanen, S. and Tittonen, I., "Towards broad-bandwidth polarization-independent nanostrip waveguide ring resonators," Opt. Express 21(8), 9974-9981 (2013).

[21] Alasaarela, T., Saastamoinen, T., Hiltunen, J., Säynätjoki, A., Tervonen, A., Stenberg, P., Kuittinen, M., and Honkanen, S., "Atomic layer deposited titanium dioxide and its application in resonant waveguide grating," Applied Optics 49(22), 4321–4325 (2010).

[22] Bradley, J. D. B., Evans, C. C., Choy, J. T., Reshef, O., Deotare, P. B., Parsy, F., Phillips, K. C., Lončar, M., and Mazur, E., "Submicrometer-wide amorphous and polycrystalline anatase TiO2 waveguides for microphotonic devices," Optics Express 20(21), 23821–23831 (2012).

[23] Furuhashi, M., Fujiwara, M., Ohshiro, T., Tsutsui, M., Matsubara, K., Taniguchi, M., Takeuchi, S. and Kawai, T., "Development of microfabricated TiO2 channel waveguides," AIP Advances 1, 032102 (2011).

[24] Mechiakh, R., Meriche, F., Kremer, R., Bensaha, R., Boudine, B., and Boudrioua, A., "TiO2 thin films prepared by sol–gel method for waveguiding applications: Correlation between the structural and optical properties," Opt. Mat. 30(4), 645–651 (2007).

[25] Bi, Z.-F., Wang, L., Liu, X.-H., Zhang, S.-M., Dong, M.-M., Zhao, Q.-Z., Wu, X. L. and Wang, K.-M., "Optical waveguides in TiO2 formed by He ion implantation.," Opt. Express 20(6), 6712–6719 (2012).

[26] Häyrinen, M., Roussey, M., Gandhi, V., Stenberg, P., Säynätjoki, A., Karvonen, L., Kuittinen, M. and Honkanen, S., "Low-loss titanium dioxide strip waveguides fabricated by atomic layer deposition," Journal of Lightwave Technology, 32(2), 208-212 (2014).

[27] Aarik, J., Aidla, A., Uustare, T. and Sammelselg, V., "Morphology and structure of TiO2 thin films grown by atomic layer deposition," Journal of Crystal Growth 148(3), 268–275 (1995).

[28] Martin, N., Rousselot, C., Rondot, D., Palmino, F. and Mercier, R., "Microstructure modification of amorphous titanium oxide thin films during annealing treatment," Thin Solid Films 300(1-2), 113–121 (1997).

[29] Ritala, M., Leskelä, M., Niinistö, L., Prohaska, T., Friedbacher, G. and Grasserbauer, M., "Surface roughness reduction in atomic layer epitaxy growth of titanium dioxide thin films," Thin Solid Films 249(2), 155–162 (1994).

[30] Maula, J., Härkönen, K., and Nikolov, A., "Multilayer material and method of preparing same," US Patent 7,901,736 (2011).

[31] Maula J., and Alasaarela, T., "METHOD FOR FORMING A DECORATIVE COATING, A COATING, AND USES OF THE SAME," US Patent Application 2012/0218638 A1 (2012).

[32] Alasaarela, T., Karvonen, L., Jussila, H., Säynätjoki, A., Mehravar, S., Norwood, R. A., Peyghambarian, N., Kieu, K., Tittonen, I., and Lipsanen, H., "High quality crystallinity controlled ALD TiO$_2$ for waveguiding applications", Optics Letters, 38(20), 3980-3983 (2013).

[33] George, S. M.,"Atomic layer deposition: an overview," Chemical Reviews, 110(1), 111-131 (2010).

[34] Kim, J., Chakrabarti, K., Lee, J., Oh, K. and Lee, C., "Effects of ozone as an oxygen source on the properties of the Al2O3 thin films prepared by atomic layer deposition," Materials Chemistry and Physics 78(3), 733–738 (2003).

[35] Elliott, S., Scarel, G., Wiemer, C., Fanciulli, M. and Pavia, G., "Ozone-based atomic layer deposition of alumina from TMA: Growth, morphology, and reaction mechanism," Chemistry of Materials 18(16), 3764–3773 (2006).

[36] Southwell, W. H., "Coating design using very thin high- and low-index layers," Appl. Opt. 24(4), 457-460 (1985).

[37] Lujala, V., Skarp, J., Tammenmaa, M. and Suntola, T., "Atomic layer epitaxy growth of doped zinc oxide thin films from organometals," Appl. Surf. Sci. 82/83, 34-40 (1994).

[38] A. Wójcik, M. Godlewski, E. Guziewicz, R. Minikayev, and W. Paszkowicz, "Controlling of preferential growth mode of ZnO thin films grown by atomic layer deposition" J. Crystalline Growth 310(2), 284-289 (2008).